Available online at www.scholarsresearchlibrary.com

Scholars Research Library

Der Pharmacia Lettre, 2016, 8 (7):119-128
(http://scholarsresearchlibrary.com/archive.html)

Scholars Research Library
ISSN 0975-5071
USA CODEN: DPLEB4

Photochemical decolorization of Methyl Violet dye using *Azadirachta indica* (Neem) mediated synthesized silver nanoparticles

***Mendhulkar Vijay D., Yadav Anu and Khamkar Supriya**

Department of Botany, Institute of Science, 15, Madam Cama Rd, Fort, Mumbai-32, Maharashtra

---

ABSTRACT

Manufacturing and use of synthetic dyes for fabric dyeing has become a massive industry. However their toxic nature has become a cause of concern. The dye industries release high content color effluents that are toxic and resistant to degradation by conventional methods. Accumulation of these dyes in water causes eutrophication reduces reoxygenation capacity and damage to the aquatic organisms by hindering the infiltration of sunlight. Here we report a green method for synthesis of silver nanoparticles using the leaf extract of Neem. The biosynthesized nanoparticles are characterized by UV-vis spectroscopy, XRD, TEM and FTIR. The AgNPs were used to degrade Methyl violet dye in the presence of sunlight. UV-visible spectra showed the maximum absorbance at 420 nm due to the excitation of surface plasmon vibrations in the AgNPs. FTIR spectrum exhibited the characteristic band at 500 cm^{-1} which is characteristic to the AgNPs. The XRD spectrum showed four different diffraction peaks corresponding to the face centered cubic (FCC) silver lines. TEM study revealed spherical AgNPs with the size range of 7-22 nm. The results of this study show the successful photodegradation of Methyl violet dye where 97% dye is degraded after 50 hours treatment.

Keywords: Ag nanoparticles, *Azadirachta indica*, dye degradation, Infrared spectrophotometer

---

INTRODUCTION

Industrial development leads to the disposal of a large number of toxic pollutants. Pollutants of any kind are degrading to the environment and hazardous to human health. It is difficult to degrade the pollutants by natural means. Dyes of all kind, be it textile dyes or other industrial dyes constitute the largest group of chemicals produced worldwide. Organic dyes are one of the major groups of pollutants widely used. The hazardous effects of organic dyes in wastewater have been a major concern. Dye effluents discharged in water bodies contaminate water and the surrounding environment. Aquatic life and the biological processes in river get affected due to this contamination. Hence, removal of dyes from industrial effluents has a great significance in connection with environmental and human health safety.

During the past decade, many methods were investigated for the degradation of dye pollutants with different methods like photo catalytic degradation [1,2], oxidative processes [3], biodegradations [4,5] etc. But these methods are time consuming and require specific conditions. The superiority of photocatalytic degradation by nanoparticles in wastewater treatment is due to reasons like quick oxidation, no formation of polycyclic products and oxidation of pollutants. It is an effective and rapid technique in the removal of pollutants from wastewater [6].

Synthesis of metal nanoparticles, their characterization and applications in many fields have become an important trend in science. Nanoparticles have unique chemical, electronic, magnetic and optical properties due to their small size and high surface area [7,8,9]. Nanoparticles have found uses in various fields such as catalysis, drug delivery system, optoelectronics, magnetic devices etc. For example, metal nanoparticles show presence of strong absorbance band in the visible region due to specific optical properties, which are not found for bulk metals. This absorbance band arises due to plasmon oscillation modes of conduction electrons [10]. Due to this plasmon band optical properties of metal particles, particularly of gold, silver and copper nanoparticles, have received considerable attention [11]. Secondly, because of their larger surface area to volume ratio and size dependent reactivity metal nanoparticles are found to be promising adsorbents and catalysts. Silver nanoparticles have shown amazing catalyst activity for various important reactions [12].

In the present investigation silver nanoparticle was chosen to study its catalytic properties in presence of an anionic dye. Methyl violet dye is used extensively in textile industries and was chosen as a model compound for photodegradation experiments. UV-visible and FTIR analysis of dye degradation directs the surface chemistry and drives the mechanistic pathway of degradation.

Nanoparticle synthesis by biological sources has been gaining great interest as they are environment friendly, non-toxic and time efficient [13]. Phytochemicals are important natural resource as they are amazing reducing agents for the phytosynthesis of metal nanoparticles. They play important roles in both stabilization and reduction of nanoparticles. The focus of the present work is to apply the accurate principles of green chemistry for the synthesis of silver nanoparticles using leaf extracts of *Azadirachta indica* as a stand-alone reducing and capping agent. Leaf extracts of *Azadirachta indica* (commonly known as neem) a species of family Meliaceae was used for bioconversion of silver ions to silver nanoparticles. This plant is commonly available in India and each part of this tree has been used as an age old remedy against various human ailments [14].

MATERIALS AND METHODS

Typically, a plant extract-mediated bioreduction involves mixing the aqueous extract with an aqueous solution of the appropriate metal salt. The synthesis of nanoparticle occurs at room temperature and completes within a few minutes.

Preparation of plant extract

A. indica leaf extract was used to prepare silver nanoparticles on the basis of cost effectiveness, ease of availability and its medicinal property. Fresh leaves of *Azadirachta indica* were collected from the Botanical garden of Vashi area, Navi Mumbai in the month of November, 2015. They were surface cleaned with running tap water to remove debris and other contaminated organic contents, followed by double distilled water and air dried at room temperature. Then plant extract was prepared by boiling 10gm of fresh neem leaves in 100ml distilled water. The solution was boiled for 20 min and then filtered using Whatman filter paper no. 1 to remove the particulate matter. The final supernatant was used for the reduction of silver ions (Ag^+) to silver nanoparticles (Ag^0).

Green synthesis of silver nanoparticles

Silver nitrate GR was purchased from Merck, India. 10 mM $AgNO_3$ solution was prepared by dissolving 169 mg of $AgNO_3$ in 100 ml distilled water, it was mixed properly to obtain clear solution. In the experimental flask 50 ml of leaf extract and 50 ml of 10 mM $AgNO_3$ solution was taken. Make the final volume to 500ml with distilled water. Mixed it well and expose the flask to sunlight to initiate the synthesis of nanoparticles. This setup was exposed to sunlight along with a negative control setup. Reduction of Ag^+ to Ag^0 was confirmed by the color change of solution from colorless to brown. Its formation was also confirmed by using UV-visible spectroscopy.

Characterization of synthesized silver nanoparticles

The optical property of AgNPs was determined by UV-Vis spectrophotometer (Model- Shimadzu UV 1800). After the addition of $AgNO_3$ to the plant extract, the spectra were taken at different time intervals up to 6hrs between 350nm to 500nm. Crystalline nature of the nanoparticles was analyzed by XRD at 2θ diffraction angle ranges from 20° to 80°. The XRD studies were conducted using Rigaku mini flex bench top X-ray spectrophotometer at The Institute of Science, Mumbai. The chemical composition of the synthesized silver nanoparticles was studied by using FTIR spectrometer (Perkin-Elmer LS-55- Luminescence spectrometer). The solutions were dried at 75^o C and

the dried powders were characterized in the range 4000–400 cm^{-1} using KBr pellet method. The particle size and surface morphology was analyzed using Transmission electron microscopy (TEM). TEM sample of the phytofabricated AgNPs was prepared by sonicating the sample in a sonicator (Vibronics VS 80) for 15 minutes. The sonicated sample was then loaded on a copper grid and allowed to dry in vacuum. TEM observations were performed on transmission electron microscope (PHILIPS model CM 200) operated at an accelerating voltage of 200 kV with the resolution of 0.22nm at the Sophisticated Analytical Instrument Facility (SAIF), Indian Institute of Technology, Powai, Mumbai.

Photocatalyic Degradation of Dye

Typically 10mg of methyl violet dye was added to 100 ml of double distilled water and used as stock solution. About 10 mg of biosynthesized silver nanoparticles was added to 100ml of methyl violet dye solution. A control was also maintained without addition of silver nanoparticles. Before exposing to sunlight/irradiation, the reaction suspension was well mixed by being magnetically stirred for 30min to clearly make the equilibrium of the working solution. Afterwards, the dispersion was put under the sunlight and monitored from morning to evening sunset. At specific time intervals, aliquots of 2-3ml suspension were filtered and used to evaluate the photocatalytic degradation of dye. The absorbance spectrum of the supernatant was subsequently measured using UV-Vis spectrophotometer at 590nm wavelength. Concentration of dye during degradation was calculated by the absorbance value at 590 nm.

Percentage of dye degradation was estimated by the following formula:

$$\% \text{ Decolorization} = \frac{100 \times (C_0 - C)}{C_0},$$

Where C_0 is the initial concentration of dye solution and C is the concentration of dye solution after photocatalytic degradation.

RESULTS AND DISCUSSION

Visual observation

Initially, while adding the leaf extract of *Azadirachta indica* to the silver salt solution, the color of the solution turned into brown which indicates the formation of silver nanoparticles [15]. It is evident from Fig-1a that the plant extract is pale yellow in color. However, the bottles containing mixture of the leaf broth with 10mM $AgNO_3$ solution turned brown-black in color within a few minutes indicating the formation of silver nanoparticles (Fig-1b). The formation of color occurred due to the excitation of surface Plasmon resonance of the silver nanoparticles [16]. The result obtained in this investigation is very interesting in terms of identification of potential plants for synthesizing the silver nanoparticles [17]. Similarly, Govindaraju *et al*., observed the color change to brownish yellow while synthesizing silver nanoparticles using the leaf extract of *Solanum torvum* [18]. Rao and Savithramma also reported that the *Svensonia hyderabadensis* solution of the silver ion complex started to change the color from yellow to dark brown due to the reduction of silver ions [19]. Chen *et al*., reported the intensity of the color development in the reaction mixture of different plants such as in *Helianthus annuus, Basella alba* and *Saccharum officinarum* [20].

Fig. 1: a- *Azadirachta indica* leaf broth, b- Silver nanoparticle formation

UV-Vis Spectrophotometer Analysis

UV-Vis spectroscopy is one of the important and simple ways to confirm the formation of nanoparticles. The shifting of absorption peak towards higher energy wavelength indicates decrease in the size of nanoparticles and vice versa. Reduction of silver ions into silver nanoparticles during exposure to plant extract was observed as a result of the color change. After addition of *Azadirachta indica* leaf extract to the aqueous solution of $AgNO_3$ of 10mM concentration, the mixture showed a gradual change in color in the presence of sunlight with time from yellowish to dark brown-black and the color intensified within 24 hours. The sharp bands of silver nanoparticles were observed around 420 nm (Fig-2). Appearance of this peak, assigned to a Surface Plasmon Resonance (SPR) band, is well-documented for various metal nanoparticles with different size range [21]. The position and shape of SPR band is dependent on the nature of the type of the material, size, geometry and the filling factor of the nanoparticle arrays, as well as the refractive index of the underlying media. The particle geometry and distribution are modified by the surface conditions provided by the dielectric layer and change in the refractive index altering the resonance position [22].

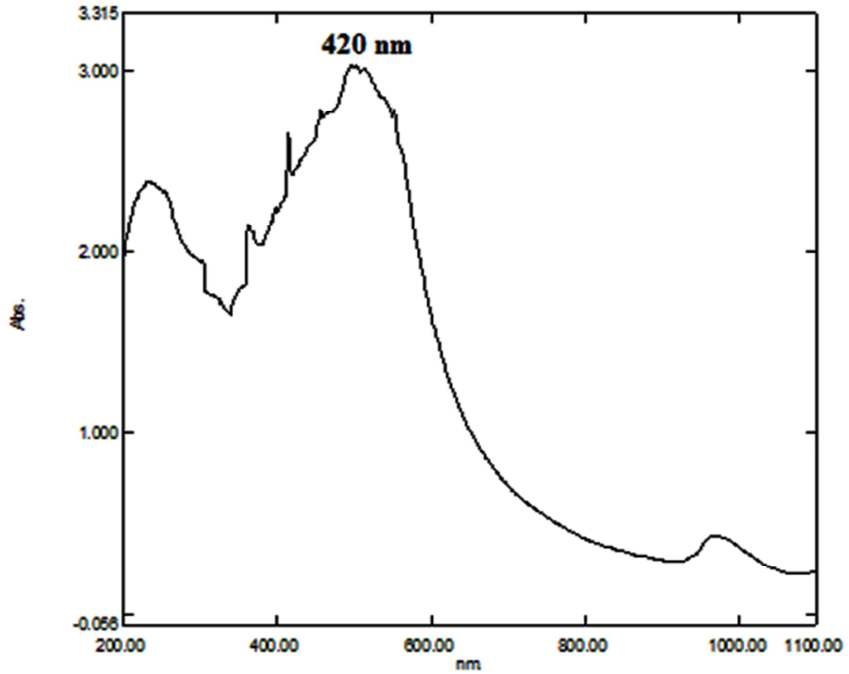

Fig. 2: The absorbance spectrum of synthesized AgNPs showing maximum absorbance at 420nm

X-Ray diffraction Analysis

The *Azadirachta indica* leaf extract-mediated synthesized Ag nanoparticle was confirmed by the characteristic peaks observed in the XRD image which is shown in Fig-3. All diffraction peaks correspond to the characteristic face centered cubic (FCC) silver lines. The XRD pattern of powder sample of phytofabricated SNPs exhibited peaks at 38°, 44°, 64° and 77°, 2θ values that indexes the (111), (200), (220) and (311) facets of silver, respectively. The XRD curve confirmed that the nanoparticles are nothing but silver. The silver nanoparticles showed the two peaks of silver at 2θ = 38° and 44° that can be assigned to the (111) and (200) facets of silver, respectively, which go very well with the values manipulated for face centered cubic structure of silver nano-crystals (according to JCPDS: File No. 04-0783).

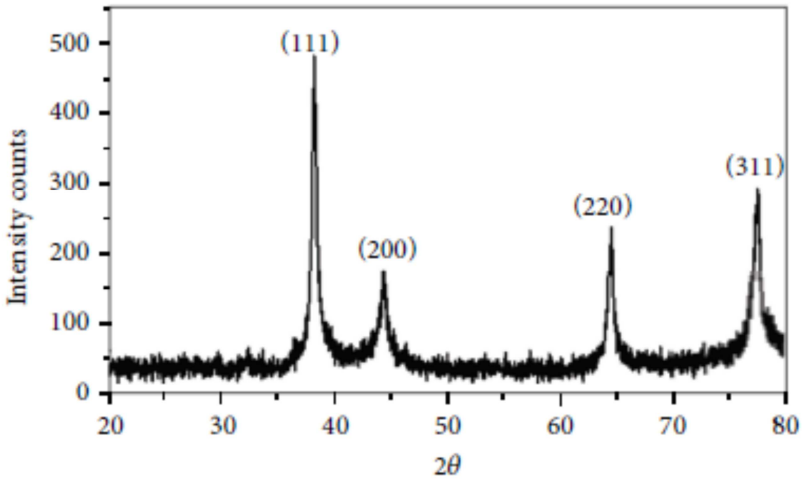

Fig. 3: XRD spectra of silver nanoparticles in *A. indica*

TEM Analysis

The TEM images of leaf mediated synthesized AgNPs are presented in Fig-4a, which gives clear indications regarding structure, shape and particle size distribution. From the images, it can be seen that the particles are covered with extract it may be the phytoconstituents of extract. TEM analysis infers the diameter of the metallic core of the nanoparticles as well as the shell around it. In some cases the shell may not be seen because the hydrate polymer shell gets collapsed in the high vacuum. No information about the state of agglomeration is obtained by electron microscopy because agglomeration may also occur during the drying process. TEM analysis of synthesized AgNPs revealed the synthesis of monodispersed spherical AgNPs with the size distribution in the range of 7-22 nm. Selected area electron diffraction (SAED) pattern obtained from AgNP (Fig-4b) showed the diffraction rings from inner to outer associated with the [111, 200, 220, 311] atomic planes of Ag indicating the formation of crystalline silver nanoparticles. A comparative analysis of the size, shape and biochemical shell around the AgNPs determined by TEM can be seen in the figure below (Fig-4a).

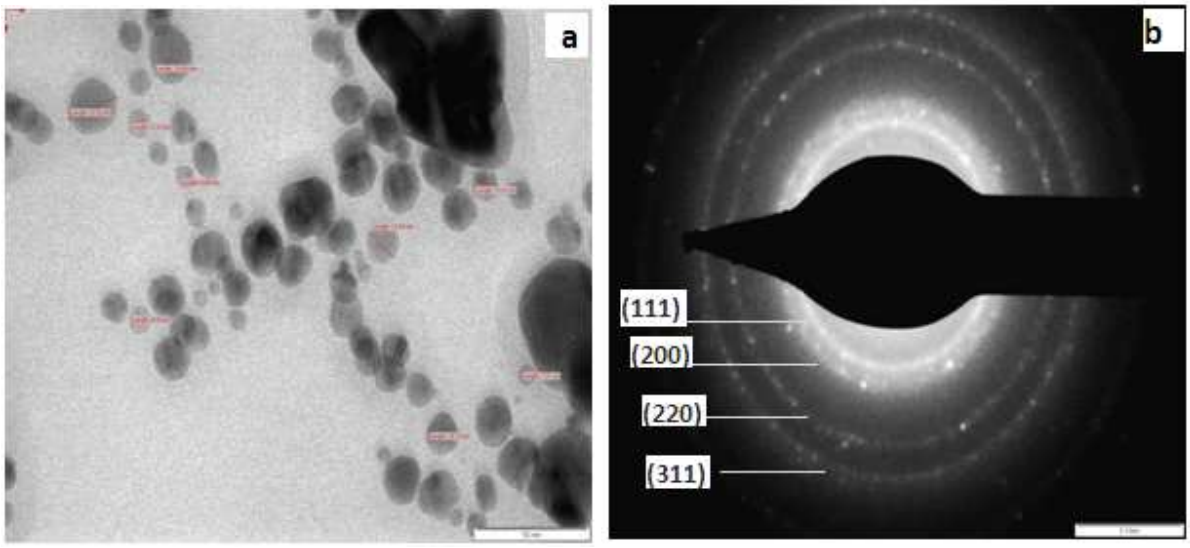

Fig. 4: TEM images of Silver nanoparticles (a) 100nm and (b) SAED of AgNPs in *A. indica*

FTIR Analysis

The functional groups present on the surface of the Ag nanoparticles were identified by FTIR analysis. The FTIR spectrum of silver nanoparticles (Fig-5) showed the band at 3305.27 cm^{-1} corresponds to O-H stretching H-bonded alcohols and phenols. The peak found around 1615.77 cm^{-1} showed a stretch for C-H bond, peak around 1408.15 cm^{-1} showed the bond stretch for N-H. The intense bands at 2924.3 and 2860.6 cm^{-1} (C-O stretch, free), 1127.59 cm^{-1} (C=C stretch) and 830.53 cm^{-1} (C-F strong stretch). Whereas, the vibration stretch for AgNPs was found at 500 cm^{-1}. Therefore, the synthesized nanoparticles were surrounded by proteins and metabolites such as terpenoids having functional groups. The presences of IR bands suggest the phenolics, alkaloids and terpenoids adsorbed on the surface of AgNPs. From the analysis of FTIR studies we confirmed that the carbonyl groups from the amino acid residues and proteins has the stronger ability to bind metal indicating that the proteins could possibly form the metal nanoparticles (i.e. capping of silver nanoparticles) to prevent agglomeration and thereby stabilize the medium. This suggests that the biological molecules could possibly perform dual functions of formation and stabilization of silver nanoparticles in the aqueous medium. The possible mechanism for the reduction of Ag^{+} to AgNPs is that phenolic OH groups present in hydrolysable tannins can form intermediate complexes with Ag^{+} ions which consequently undergo oxidation to quinone forms with subsequent reduction of Ag^{+} to Ag nanoparticles [23].

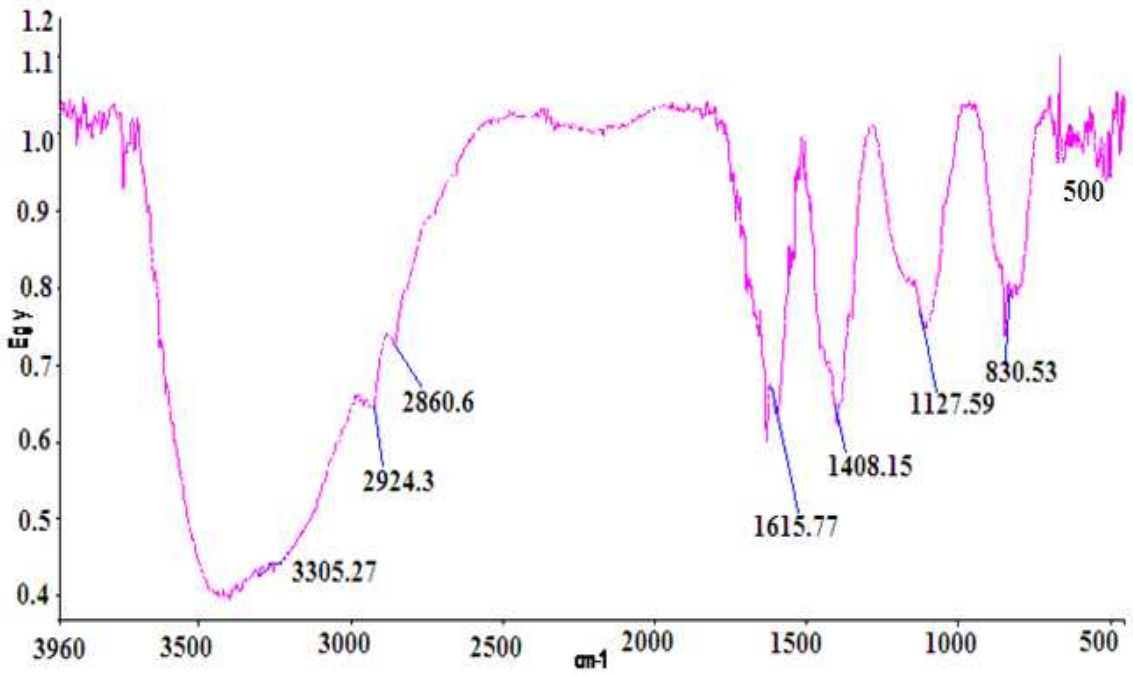

Fig. 5: FTIR spectra of silver nanoparticles synthesized using *Azadirachta indica* leaf extract

Photocatalytic Degradation of Dye

Visual Observation

Photocatalytic degradation of methyl violet was carried out using green synthesized silver nanoparticles under solar light. Dye degradation was initially identified by color change. Initially, the color of dye shows deep violet color, after exposure to sunlight the color changed to light blue after 1 hour of incubation with silver nanoparticles (Fig-6). Subsequently light blue was changed to faint violet. Finally, the degradation process was completed at 48 hr and was identified by the change of reaction mixture from violet color to almost colorless.

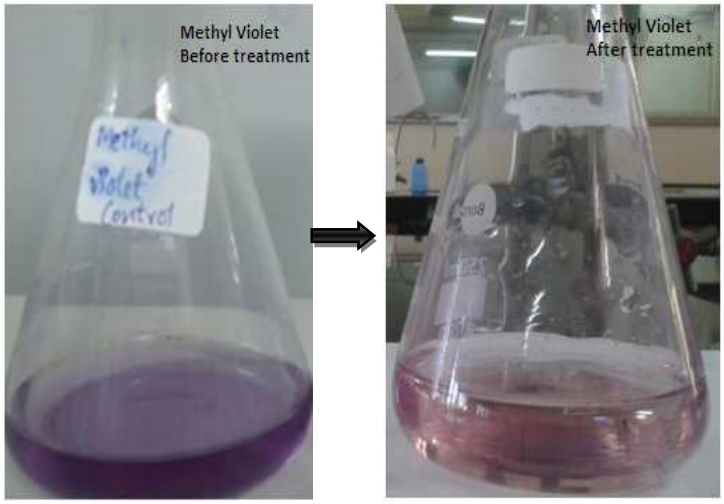

Fig. 6: Visual observation of color change indicating dye degradation

Kinetic experiments

Photocatalytic activity of silver nanoparticles on degradation of dye was demonstrated using the dye methyl violet. The degradation of methyl violet was carried out in the presence of silver nanoparticles at different time in the visible region. The absorption spectrum showed the decreased peaks for methyl violet at different time intervals. Initially, the absorption peaks at 590 nm for methyl violet dye were decreased gradually with the increase of the exposure time and that indicates the photocatalytic degradation reaction of methyl violet. The absorption peak of methyl violet dye was decreased. The completion of the photocatalytic degradation of the dyes is known from the gradual decrease of the absorbance value of dye approaching the base line. The percentage of degradation efficiency of silver nanoparticles was calculated as 97.09% at 50hr (Table-1). The degradation percentage was increased as increasing the exposure time of dye silver nanoparticles complex in sunlight (Fig-7). Absorption peak for methyl violet dye was centered at 590 nm in visible region which diminished and finally it disappeared while increasing the reaction time, which indicates that the dye had been degraded.

Table 1: Methyl violet degradation (%) by synthesized silver nanoparticles (10mg)

Exposure Time (Hours)	Amount of degradation of dye (%)
1	29.55
2	42.21
3	46.70
4	58.83
5	66.49
24	84.69
25	87.59
26	89.97
27	92.34
28	94.98
48	96.04
50	97.09

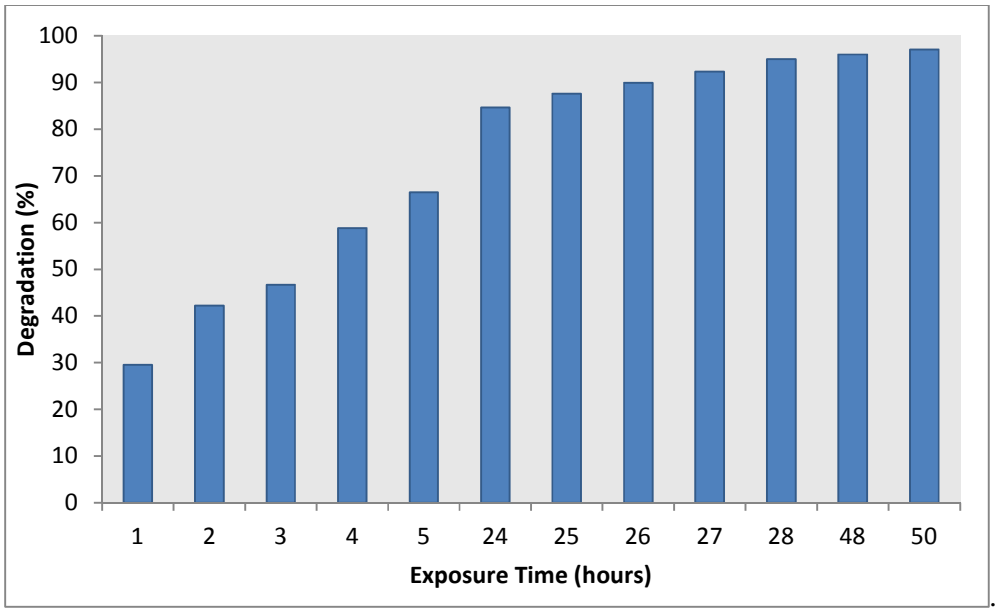

Fig. 7: Percentage of dye degradation by 10mg of synthesized silver nanoparticles at different functional time intervals

Infrared spectrometric evaluation for decolorization of dye

The FTIR spectra of control Methyl violet (Fig-8A), displays a peak at 3749.34 cm^{-1} for asymmetric O-H stretching vibrations; peak at 3335.10 cm^{-1} for C-H vibration; peaks at 1,544.29 and 1,431.93 cm^{-1} for the C = C–H in plane C–H bend and $–CH_3$ vibrations, respectively; peak at 1,108.3 for –S=O bond; and a peak at 838.73 cm^{-1} for the 1, 4 di-substituted (Para) benzene ring. The peak at 1621.88 cm^{-1} is due to aromatic C=C bond. All these peaks confirm the aromatic nature of the dye. But in Fig-8B the peaks between 3700-1650 cm^{-1} indicating aromatic bond and

phenyl ring substitution band, peak at 1431.93 cm^{-1} indicating methyl group vibrations (-CH_3) is totally absent and benzene ring at 838.73 cm^{-1} was entirely absent. The FTIR spectrum of the degradation products formed by degradation due to AgNPs had displayed entirely new peaks (Fig-8B) compared to the initial control dye (Fig-8A), which confirms the degradation of Methyl violet. The new peak at 1632.4 cm^{-1} correspond to the N-H stretch and asymmetrical stretch of nitro compounds (C=N). Another peak at 1112.6 cm^{-1} corresponds to the C-O bond. During the degradation process, bands of vibrations characteristic of the carbon-hydrogen bond, the O-H bond, the sulphate bond, and nearly all of the aromatic skeletal vibrations decreased and disappeared. Meanwhile, some new IR absorption bands appeared in the region 900-650 cm^{-1} indicating a non-aromatic structure of the band. This indicates that silver nanoparticle used in the present experiment in presence of sunlight had resulted in the degradation of the dye to form new products.

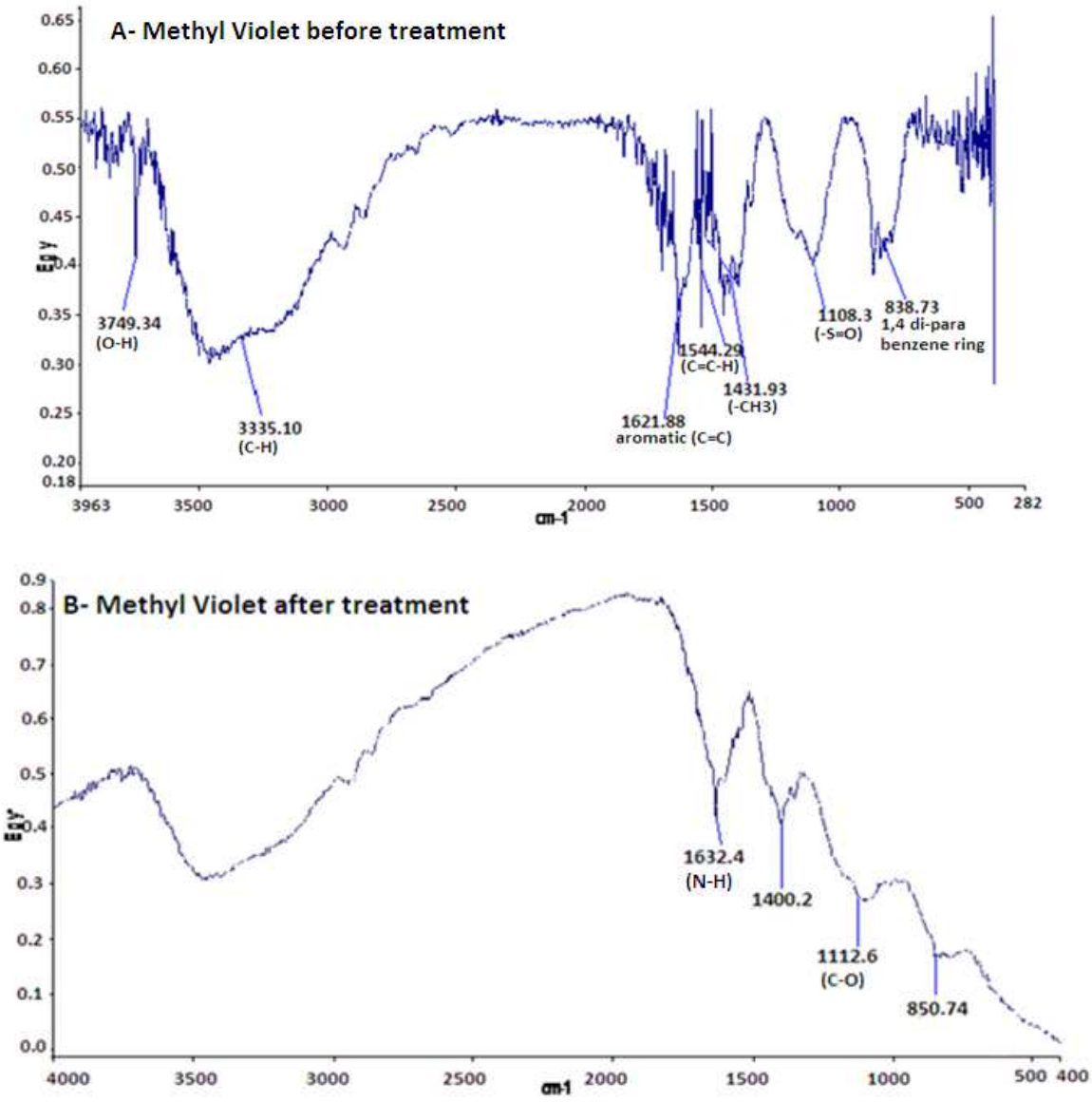

Fig.8- Infrared spectra of Methyl Violet dye before and after decolorization studies with photo-catalyzed AgNPs

CONCLUSION

Green nanotechnology is gaining importance due to the elimination of harmful reagents and provides effective synthesis of expected products in an economical manner. Green synthesis of silver nanoparticles shows more compatible, ecofriendly, low cost, and less time consuming process. Herein, the silver nanoparticles were synthesized using plant leaf extract of *Azadirachta indica*. UV-visible spectroscopy confirmed the formation of silver nanoparticles and the absorption maxima spectra was observed at 420 nm. Spherical shape of the nanoparticles with the size ranges from 7 to 23nm was confirmed by TEM analysis. Crystalline nature was characterized by the X-ray diffraction analysis. The photocatalytic activity of green synthesized silver nanoparticles was evaluated on methyl violet dye. The main absorption peak at 590 nm of methyl violet dye decreased gradually with the extension of the exposure time indicating the photocatalytic degradation of methyl violet dye. 97% degradation of methyl violet dye was completed within 50 hours. FTIR spectra revealed the photodegradation of the methyl violet dye after 24 hours treatment with AgNPs. The elimination of peaks of spectra for methyl group and benzene ring (characterized component) was clearly evident in infrared spectrometric analysis. In the present study, it is found that the use of natural renewable and eco-friendly reducing agent used for synthesis of silver nanoparticles exhibits excellent photocatalytic activity against dye molecules and can be used in water purification systems and dye effluent treatment.

Acknowledgement
The authors are thankful to the Department of Chemistry, Institute of Science for providing with XRD and FTIR analysis; Head, Department of Botany, Institute of Science, Mumbai for UV-vis spectroscopy, and Sophisticated Analytical Instrument Facility, IIT, Mumbai for TEM analysis.

REFERENCES

[1] Liu G, Zhao J, *New Journal of Chemistry*, **2000**, 24, 411-417.
[2] Vinodgopal K, Kamat P.V, *Environmental Science and Technology*, **1995**, 29(3), 841-845.
[3] Hammami S, Oturan N, Bellakhal N, Dachraoui M, Oturan M.A, *Journal of Electroanalytical Chemistry*, **2007**, 610(1), 75-84.
[4] Carias C.C, Novais J.M, Martins-Dias S, *Bioresource Technology*, **2008**, 99(2), 243–251.
[5] Jadhav U.U, Dawkar V.V, Ghodake G.S, Govindwar S.P, *Journal of Hazardous Materials*, **2008**, 158(2–3), 507–516.
[6] Sobana N, Muruganadham M, Swaminathan M, *Journal of Molecular Catalysis A*, **2006**, 258, 124–132.
[7] Hodak J.H, Martini I, Hartland G.V, *The Journal of Physical Chemistry B*, **1998**, 102(36), 6958-6967.
[8] Kamat P.V, Flumiani M, Hartland G.V, *The Journal of Physical Chemistry B*, **1998**, 102(17), 3123-3128.
[9] Logunov S.L, Ahmadi T.S, El. Sayed M.A, Khoury J.T, Whetten R.L, *The Journal of Physical Chemistry*, **1997**, 101(19), 3713–3719.
[10] Hodak J.H, Henglein A, Hartland G.V, *Pure and applied chemistry*, **2000**, 72(1-2), 189-197.
[11] Fujiwara H, Yangida S, Kamat P.V, *The Journal of Physical Chemistry B*, **1999**, 103, 2589-2591.
[12] Pradhan N, Pal A, Pal T, *Langmuir*, **2001**, 17(5), 1800-1802.
[13] Patil R.S, Kokate M.R, Kolekar S.S, *Spectrochimica Acta A*, **2012**, 91, 234–238.
[14] Omoja V.U, Anaga A.O, Obidike I.R, Ihedioha T.E, Umeakuana P.U, Mhomga L.I, Asuzu I.U, Anika S.M, *Asian Pacific Journal of Tropical Medicine*, **2011**, 4(5), 337-341.
[15] Sastry M, Patil V, Sainkar S.R, *Journal of Physical Chemistry B*, **1998**, 102(8), 1404–1410.
[16] Mulvaney P, Langmuir, **1996**, 12(3), 788–800.
[17] Prasad T.N.V.K.V, Elumalai E.K, *Asian Pacific Journal of Tropical Biomedicine*, **2011**, 1(6), 439–442.
[18] Govindaraju K, Tamilselvan S, Kiruthiga V, Singaravelu G, *Journal of Biopesticides*, **2010**, 3(1), 394–399.
[19] Rao M.L, Savithramma N, *Journal of Pharmaceutical Sciences and Research*, **2011**, 3(3), 1117–1121.
[20] Chen S, Webster S, Czerw R, Xu J, Carroll D.L, *Journal of Nanoscience and Nanotechnology*, **2004**, 4(3), 254–259.
[21] Muthukrishnan S, Bhakya S, Kumar T.S, Rao M.V, *Industrial Crops and Products*, **2015**, 63, 119-124.
[22] Raut R, Lakkakula J, Kolekar N, Mendhulkar V.D, Kashid S, *Current Nanoscience*, **2009**, 5, 117-122.
[23] Fayaz A.M, Balaji K, Girilal M, Yadav R, Kalaichelvan P.T, Venketesan R, *Nanomedicine*, **2010**, 6, 103-109.